

# AMP kinase–mediated activation of the BH3-only protein Bim couples energy depletion to stress-induced apoptosis

Caoimhín G. Concannon,<sup>1,2</sup> Liam P. Tuffy,<sup>1,2</sup> Petronela Weisová,<sup>1,2</sup> Helena P. Bonner,<sup>1,2</sup> David Dávila,<sup>1,2</sup> Caroline Bonner,<sup>1,2</sup> Marc C. Devocelle,<sup>3</sup> Andreas Strasser,<sup>4</sup> Manus W. Ward,<sup>1,2</sup> and Jochen H.M. Prehn<sup>1,2</sup>

<sup>1</sup>Department of Physiology and Medical Physics, <sup>2</sup>Neuroscience Research Centre, Royal College of Surgeons in Ireland (RCSI) Research Institute, and <sup>3</sup>Department of Pharmaceutical and Medicinal Chemistry, RCSI, Dublin 2, Ireland

<sup>4</sup>Molecular Genetics of Cancer Division, Walter and Eliza Hall Institute of Medical Research, Parkville, Victoria 3052, Australia

**E**xcitotoxicity after glutamate receptor overactivation induces disturbances in cellular ion gradients, resulting in necrosis or apoptosis. Excitotoxic necrosis is triggered by rapid, irreversible ATP depletion, whereas the ability to recover cellular bioenergetics is suggested to be necessary for the activation of excitotoxic apoptosis. In this study, we demonstrate that even a transient decrease in cellular bioenergetics and an associated activation of adenosine monophosphate–activated protein kinase (AMPK) is necessary for the activation of excitotoxic apoptosis. We show that the Bcl-2 homology domain 3 (BH3)–only

protein Bim, a proapoptotic Bcl-2 family member, is activated in multiple excitotoxicity paradigms, mediates excitotoxic apoptosis, and inhibits delayed Ca<sup>2+</sup> deregulation, mitochondrial depolarization, and apoptosis-inducing factor translocation. We demonstrate that *bim* activation required the activation of AMPK and that prolonged AMPK activation is sufficient to induce *bim* gene expression and to trigger a *bim*-dependent cell death. Collectively, our data demonstrate that AMPK activation and the BH3-only protein Bim couple transient energy depletion to stress-induced neuronal apoptosis.

## Introduction

The overexcitation of glutamate receptors, in particular *N*-methyl-D-aspartic acid (NMDA) receptors, has been implicated in the neuronal injury associated with ischemic stroke, head trauma, hypoglycemia, and prolonged seizures (Choi and Rothman, 1990) and may play an important role in chronic neurodegenerative disorders such as amyotrophic lateral sclerosis (Rothstein et al., 1990) and Parkinson's disease (Turski et al., 1991). Depending on intensity, duration, and intrinsic factors, an exposure of neurons to glutamate or NMDA can cause a rapid, necrotic death or a more delayed apoptotic injury characterized by cell

shrinkage and nuclear condensation (Ankarcrona et al., 1995; Lankiewicz et al., 2000; Ward et al., 2006).

Glutamate receptor overactivation leads to a massive disturbance of cellular ion homeostasis resulting from the primary or secondary influx of Na<sup>+</sup>, Ca<sup>2+</sup>, H<sup>+</sup>, and Cl<sup>−</sup> into the cytoplasm (Choi, 1987). Neurons attempt to restore their cellular ion homeostasis via the activity of ATP-consuming ion pumps, including Ca<sup>2+</sup> ATPases and the plasma membrane Na<sup>+</sup>K<sup>+</sup>ATPase, the driving force for Na<sup>+</sup>-Ca<sup>2+</sup> and Na<sup>+</sup>-H<sup>+</sup> exchangers (Brines and Robbins, 1992; Mironov, 1995). Importantly, the extent of ATP depletion and recovery of cellular bioenergetics critically determines the type of cell death that occurs (Ankarcrona et al., 1995; Bonfoco et al., 1995; Luetjens et al., 2000; Ward et al., 2000). If the extent of ionic disturbances exceeds the capacity of the ATP-dependent ion pumps to restore ionic gradients, rapid cell swelling and necrosis occurs (Ankarcrona et al., 1995;

C.G. Concannon and L.P. Tuffy contributed equally to this paper.

Correspondence to Jochen H.M. Prehn: prehn@rcsi.ie

Abbreviations used in this paper: AICAR, 5-aminoimidazole-4-carboxamide riboside; AIF, apoptosis-inducing factor; AMPK, AMP-activated protein kinase; ANOVA, analysis of variance; BH3, Bcl-2 homology domain 3; CA-AMPK, constitutively active AMPK- $\alpha$ 1; CaMKK- $\beta$ , Ca<sup>2+</sup>/calmodulin-dependent kinase kinase  $\beta$ ; CGN, cerebellar granular neuron; DCD, delayed Ca<sup>2+</sup> deregulation; DIV, day in vitro; HPLC, high performance liquid chromatography; NMDA, *N*-methyl-D-aspartic acid; OHSC, organotypic hippocampal slice culture; PI, propidium iodide; PTP, permeability transition pore; qPCR, quantitative PCR; TMRM, tetramethyl rhodamine methyl ester; WT, wild type.

© 2010 Concannon et al. This article is distributed under the terms of an Attribution–Noncommercial–Share Alike–No Mirror Sites license for the first six months after the publication date (see <http://www.rupress.org/terms>). After six months it is available under a Creative Commons License (Attribution–Noncommercial–Share Alike 3.0 Unported license, as described at <http://creativecommons.org/licenses/by-nc-sa/3.0/>).

Bonfoco et al., 1995; Ward et al., 2000, 2007). Conversely, if the ATP demand is less severe and the capacity of cells to generate ATP is sufficient, neurons restore their ionic gradients, and only a transient decrease in mitochondrial membrane potential ( $\Delta\psi_m$ ) or cellular ATP levels can be detected. Nevertheless, many of these neurons proceed to undergo apoptotic death over the following hours (Ankarcrona et al., 1995; Bonfoco et al., 1995; Luetjens et al., 2000; Ward et al., 2007).

What remains largely unresolved is the question of how excitotoxicity triggers apoptosis despite the apparent recovery of ATP levels and ionic gradients. Clearly, several pathways may be activated by the influx of  $Ca^{2+}$ , which triggers non-necrotic cell death, including the activation of nitric oxide synthase, PARP (poly[ADP-ribose] polymerase), or calpains (Dawson et al., 1991; Mandir et al., 2000). In contrast, provision of energy substrates such as glucose or pyruvate potently inhibits excitotoxic cell death (Ruiz et al., 1998; Vergun et al., 2003; Weisová et al., 2009). Evidently, energy stress induced by excitotoxins may cooperate with other cell death pathways or may even be the key stress signal for the activation of excitotoxic apoptosis. In this context, we recently demonstrated that the ability of cells to recover their bioenergetics critically determined the levels of excitotoxic apoptosis and defined a role for increased glucose uptake in this process (Ward et al., 2007; Weisová et al., 2009).

Apoptotic signaling pathways require the activation of the proapoptotic Bcl-2 family members Bax or Bak (Wei et al., 2001), resulting in the permeabilization of the outer mitochondrial membrane and the release of the intermembrane proteins, including cytochrome *c* and apoptosis-inducing factor (AIF). The transcriptional induction and/or the posttranslational activation of Bcl-2 homology domain 3 (BH3)-only proteins is believed to be essential for Bax/Bak activation and downstream signaling events. Previous studies have demonstrated that apoptotic excitotoxic injury is inhibited by loss of Bax or Bcl-2 overexpression (Xiang et al., 1998; Wang et al., 2004; Dietz et al., 2007; Semenova et al., 2007). In this study, we demonstrate that, in contrast to currently held views, ATP depletion and energy stress signaling are not only responsible for the activation of necrotic but also for the activation of apoptotic excitotoxic injury and that this occurs via the activation of an AMP-activated protein kinase (AMPK), culminating in the activation of the BH3-only protein Bim.

## Results

### Excitotoxic apoptosis activates the BH3-only protein Bim

Glutamate receptor overactivation induces a necrotic or apoptotic cell death, depending on the duration of receptor stimulation and magnitude of intracellular  $Ca^{2+}$  and  $Na^+$  loading (Ankarcrona et al., 1995). Stimulation of glutamate receptors in cerebellar granular neurons (CGNs) with 100  $\mu$ M glutamate/10  $\mu$ M Gly for 10 min resulted in a delayed excitotoxic apoptosis within a 4–24-h time frame, which was characterized by cell shrinkage and nuclear pyknosis (Fig. 1, A–C; Ward et al., 2006; Weisová et al., 2009). Glutamate excitation

resulted in an initial increase in intracellular  $Ca^{2+}$  that quickly returned to baseline levels; however, cells undergoing excitotoxic apoptosis displayed a delayed  $Ca^{2+}$  deregulation (DCD) within 10–18 h of stimulation (Fig. 1 D). Analysis of  $\Delta\psi_m$  using tetramethyl rhodamine methyl ester (TMRM) and ATP levels revealed a membrane potential depolarization during glutamate exposure that was coupled to a reduction in cellular ATP levels. Both processes were transient in nature, with TMRM fluorescence and ATP levels recovering within 1–2 h (Fig. 1, E and F). Collectively, these data suggested that glutamate receptor activation induced a transient depletion of energy levels that was followed by a delayed apoptotic response in the majority of neurons. To investigate potential mediators of this event, we used real-time quantitative PCR (qPCR) to investigate the expression levels of BH3-only proteins that have been shown to be central in coupling stress signaling to apoptotic pathways (Youle and Strasser, 2008). The mRNA expression of *bim* was significantly increased in the time frame after glutamate receptor activation, before the major increase in cell death (Fig. 1, G and H). In contrast, the expression levels of the other major BH3-only proteins, including *bid*, *puma*, and *bmf*, were not significantly altered (Fig. 1 G), suggesting that Bim may be specifically activated in response to glutamate receptor activation.

### Bim mediates excitotoxic apoptosis

Using siRNA to inhibit the expression of *bim*, we assessed the ability of CGNs to undergo cell death after glutamate excitation. As demonstrated in Fig. 1 I, *bim* siRNA significantly reduced the expression of Bim protein, as assessed by Western blotting. Importantly, the decreased expression of Bim within these neurons significantly reduced the number of neurons undergoing glutamate-induced apoptosis (Fig. 1 J).

To exclude potential off-target effects of *bim* siRNA in the protection against excitotoxic apoptosis, we availed of a panel of gene-targeted mice deficient for various BH3-only proteins (Bouillet et al., 1999; Villunger et al., 2003; Kaufmann et al., 2007). Neocortical neurons were exposed to 100  $\mu$ M NMDA for 5 min, as NMDA receptors predominantly mediate glutamate excitotoxicity in cortical neurons (Choi et al., 1987). Pyknotic nuclei were detected in the majority of neurons 24 h after excitation (Fig. 2 A), and quantification revealed a time-dependent increase in the number of pyknotic nuclei at 16 and 24 h after NMDA excitation (Fig. S1). Indeed, parallel assessment of apoptosis by propidium iodide (PI) staining revealed that the number of PI-positive cells after transient NMDA receptor activation closely paralleled apoptotic levels, as assessed by the quantification of pyknotic nuclei (Fig. S1). Analysis of the expression of the BH3-only proteins Bim, Bid, and PUMA revealed an early and sustained increase in the expression of Bim, whereas the expression of PUMA or Bid remained unchanged (Fig. 2 B). No evidence for increased cleavage of Bid into its more potent truncated form, tBid, was observed (Fig. 2 B). We next quantified the levels of pyknotic nuclei after NMDA excitation in neurons from *puma*-, *bid*-, or *bim*-deficient mice.

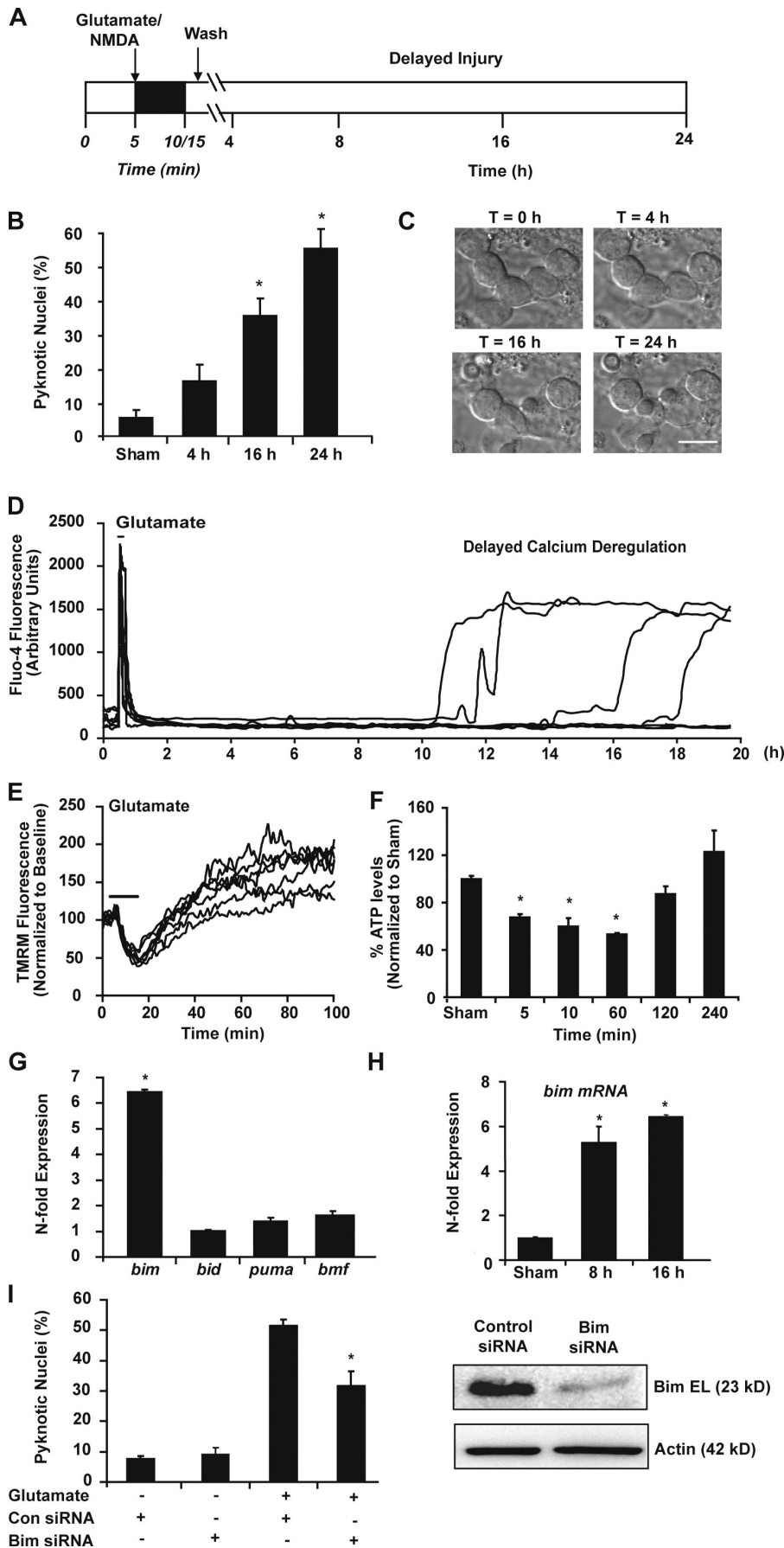
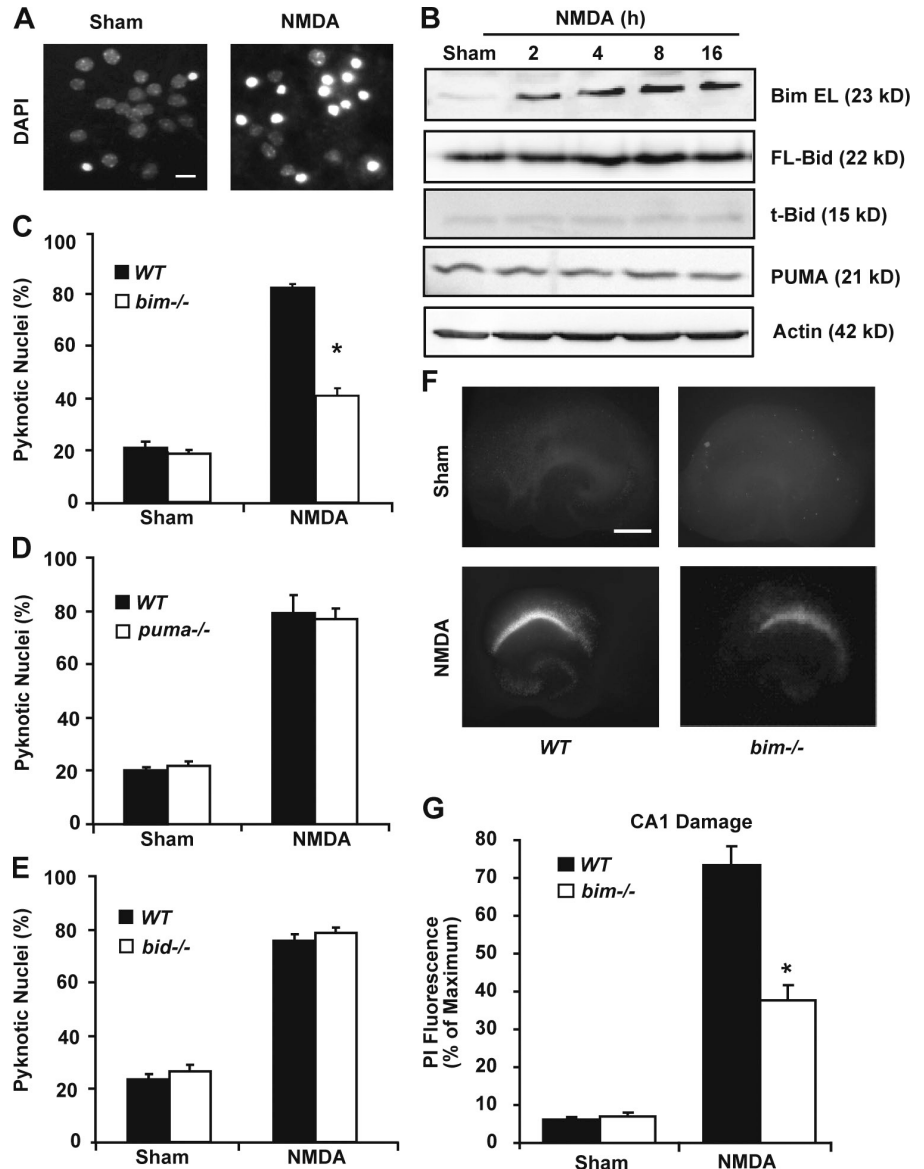


**Figure 1. NMDA receptor overactivation results in a transient depletion of ATP and delayed apoptosis associated with induction of the BH3-only protein Bim.** (A) Model of transient NMDA receptor activation. CGNs were treated with 100  $\mu$ M glutamate/10  $\mu$ M Gly for 10 min, or mouse neocortical neurons were treated with 100  $\mu$ M NMDA/10  $\mu$ M Gly for 5 min. The onset of injury occurs over a time frame of 4–24 h. (B) Time course of delayed excitotoxic apoptosis. CGNs were treated with 100  $\mu$ M glutamate/10  $\mu$ M Gly for 10 min and subsequently stained with Hoechst, and condensed pyknotic nuclei were quantified at the indicated time points. (C) Cell shrinkage during excitotoxic apoptosis. Differential interference contrast images of CGNs at the indicated time points after glutamate treatment. (D) Excitotoxic apoptosis is associated with a DCD.  $Ca^{2+}$  levels were monitored with Fluo-4 and time-lapse microscopy after treatment with 100  $\mu$ M glutamate/10  $\mu$ M Gly for 10 min. (E) Individual traces of TMRM fluorescence changes in CGNs as monitored using time-lapse microscopy after treatment with 100  $\mu$ M glutamate/10  $\mu$ M Gly for 10 min. (F) Cellular ATP levels in CGNs after treatment with 100  $\mu$ M glutamate/10  $\mu$ M Gly for 10 min. ATP levels were normalized to sham-treated neurons. (B and F) Data represent means  $\pm$  SEM from  $n = 4$  cultures. These experiments were repeated twice with similar results. \*,  $P < 0.05$  compared with sham-treated controls. (G) Real-time qPCR analysis of expression of *bim*, *bmf*, *puma*, and *bid* mRNA at 16 h after glutamate treatment relative to  $\beta$ -actin mRNA levels. (H) Real-time qPCR analysis of *bim* mRNA expression after glutamate treatment at 16 and 24 h after excitation relative to  $\beta$ -actin mRNA levels. (G and H) Expression levels were normalized to sham-treated cells, and data are represented as means  $\pm$  SEM from  $n = 3$  independent cultures. \*,  $P < 0.05$  compared with sham-treated controls. (I) CGNs transfected with control or *bim* siRNA for 72 h and subsequently treated with 100  $\mu$ M glutamate/10  $\mu$ M Gly for 10 min. Condensed pyknotic nuclei were quantified 24 h after excitation. Data represent means  $\pm$  SEM from  $n = 4$  cultures. \*,  $P < 0.05$ . This experiment was repeated once with similar results. (right) The expression levels of Bim were assessed by Western blotting 72 h after siRNA transfection. Probing for  $\beta$ -actin served as a loading control. Bar, 10  $\mu$ m.

**Figure 2. Proapoptotic BH3-only protein Bim is essential for NMDA-mediated excitotoxic apoptosis.**

(A) Neocortical neurons were exposed to 100  $\mu$ M NMDA/10  $\mu$ M Gly or sham conditions for 5 min and allowed to recover for 24 h. Nuclear morphology was assessed by Hoechst staining. (B) Neocortical neurons were treated as described in A and allowed to recover for the indicated times. The expression of the BH3-only proteins Bim, Bid, and PUMA was analyzed by Western blotting. Probing for  $\beta$ -actin served as loading control. (C–E) Mouse neocortical neurons from *bim*<sup>-/-</sup> (C), *puma*<sup>-/-</sup> (D), or *bid*<sup>-/-</sup> (E) mice and WT controls were treated with 100  $\mu$ M NMDA or sham conditions for 5 min and scored for pyknotic nuclei 24 h after excitation. Three subfields containing  $\sim$ 300 neurons each were captured and quantified per well. Data represent means  $\pm$  SEM from *n* = 4 cultures. This experiment was repeated three times with similar results. \*, *P* < 0.05 compared with NMDA-treated WT controls. (F) Representative images of OHSCs treated with 50  $\mu$ M NMDA or exposed to sham conditions for 30 min and allowed to recover for 24 h. Cell death was assessed by PI staining. (G) Quantification of cell death. OHSCs were treated as described in F, and cell death was assessed by PI staining. Experiments were performed in triplicate in three separate cultures for each strain of mice. Mean  $\pm$  SEM is shown. \*, *P* < 0.05 compared with NMDA-treated WT controls (ANOVA post-hoc Tukey). Bars: (A) 10  $\mu$ m; (F) 500  $\mu$ m.



Loss of either *bid* or *puma* expression afforded no protection after NMDA treatment (Fig. 2, D and E); however, *bim*<sup>-/-</sup> neurons provided significant protection (Fig. 2 C). We also investigated the role of Bim during excitotoxic injury in the more complex environment of mouse organotypic hippocampal slice cultures (OHSCs). Treatment with 50  $\mu$ M NMDA for 30 min resulted in cell death at the CA1 region, as assessed by PI uptake after 24 h (Fig. 2 F). This injury was accompanied by a significant induction of *bim* mRNA and Bim protein expression (Fig. S2), with loss of Bim expression affording significant protection from NMDA-induced excitotoxic injury (Fig. 2, F and G).

#### ***bim* is required for DCD and AIF translocation during excitotoxic apoptosis**

The aforementioned experiments suggested that Bim plays a key role in mediating apoptosis in multiple models of excitotoxic injury. Previous studies have indicated important roles for DCD, delayed  $\Delta\psi_m$  depolarization, and mitochondrial

outer membrane permeabilization in excitotoxic apoptosis (Ankarcrona et al., 1995; Budd et al., 2000; Luetjens et al., 2000; Ward et al., 2000, 2006; Wang et al., 2004; Cheung et al., 2005). We next investigated whether the loss of Bim expression modulated these events. Real-time imaging experiments demonstrated that the acute  $Ca^{2+}$  responses during NMDA exposure were comparable between wild-type (WT) and *bim*<sup>-/-</sup> neurons (Fig. 3, A–C). However, analysis of DCD revealed that *bim*-deficient neurons maintained their  $Ca^{2+}$  homeostasis for longer periods and underwent DCD at a much lower frequency than their WT counterparts (Fig. 3 D). Furthermore, *bim*<sup>-/-</sup> neurons maintained their  $\Delta\psi_m$  considerably longer than their WT littermates after NMDA receptor activation (Fig. 3 E). Indeed the frequency of delayed  $\Delta\psi_m$  depolarization was dramatically reduced in *bim*-deficient mice (Fig. 3 F). Cultures from *bim*-deficient mice also showed a significant reduction in the number of neurons that displayed nuclear localization of the mitochondrial protein AIF after NMDA excitation (Fig. 3, G and H).



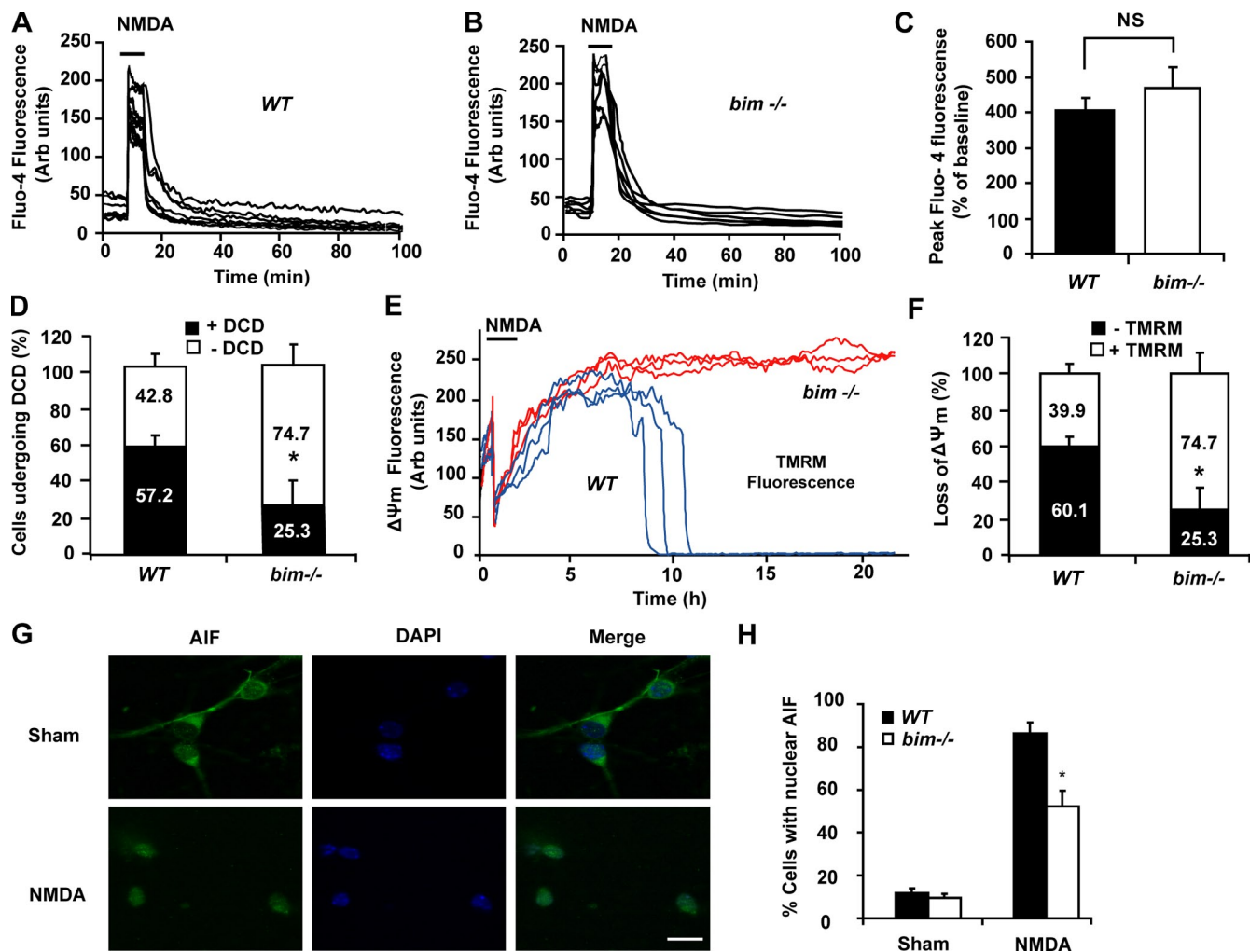


**Figure 3. Bim is required for DCD, mitochondrial depolarization, and AIF translocation during excitotoxic apoptosis.** Cortical neurons cultured on Wilco dishes were loaded with Fluo-4 AM and TMRM for 30 min at 37°C before being mounted on a thermostatic chamber of a confocal microscope. The neurons were exposed to 100  $\mu$ M NMDA/10  $\mu$ M Gly or sham conditions for 5 min, after which neuronal injury was monitored over a 24-h period. (A and B) Individual traces of initial  $\text{Ca}^{2+}$  responses in WT (A) and *bim*<sup>-/-</sup> (B) neurons after NMDA receptor activation. (C) Quantification of peak initial Fluo-4 fluorescence in WT ( $n = 91$ ) and *bim*<sup>-/-</sup> ( $n = 70$ ) neurons revealed no significant differences between genotypes. (D) Analysis of the frequency of WT ( $n = 90$ ) and *bim*<sup>-/-</sup> ( $n = 70$ ) neurons undergoing DCD. \*,  $P < 0.05$  compared with WT-treated neurons. (E) Individual traces of TMRM fluorescence in WT and *bim*<sup>-/-</sup> neurons after NMDA treatment. (F) Analysis of the frequency of WT ( $n = 91$ ) and *bim*<sup>-/-</sup> ( $n = 70$ ) neurons undergoing loss of TMRM fluorescence. \*,  $P < 0.05$  compared with WT-treated neurons. (C, D, and F) Mean  $\pm$  SEM is shown. (G) Representative images of AIF immunofluorescence in NMDA- or sham-treated cultures. (H) Quantification of the number of neurons with nuclear-localized AIF as analyzed by immunofluorescence. Mouse cortical neurons from WT and *bim*<sup>-/-</sup> mice were treated with 100  $\mu$ M NMDA/10  $\mu$ M Gly or sham conditions for 5 min and allowed to recover for 16 h. Six subfields containing  $\sim 50$  neurons each were captured and quantified for AIF release per culture. Data represent mean  $\pm$  SEM from  $n = 4$  cultures. The experiment was repeated twice with similar results. \*,  $P < 0.05$  compared with NMDA-treated WT neurons (ANOVA post-hoc Tukey). Bar, 10  $\mu$ m.

### Prolonged activation of AMPK is sufficient for increased Bim expression

Given that glucose or energy substrate supplementation inhibits excitotoxic injury (Vergun et al., 2003; Weisová et al., 2009), we tested the hypothesis that transient energy depletion in response to glutamate or NMDA mediates the activation of excitotoxic apoptosis. Similar to CGNs exposed to glutamate (Fig. 1 F), ATP levels were transiently decreased in neocortical neurons exposed to NMDA (Fig. 4 A). High performance liquid chromatography (HPLC) analysis demonstrated that the decline in cellular ATP was accompanied by an accumulation of AMP (Fig. 4 B). In both excitotoxicity models, these bioenergetic alterations correlated with increased phosphorylation of AMPK at Thr172, which is indicative of AMPK activation

(Fig. 4, C and D). To assess whether AMPK activation was sufficient to mediate neuronal apoptosis, we directly activated AMPK activity using 5-aminoimidazole-4-carboxamide riboside (AICAR), which is an AMP mimetic. The addition of AICAR to cultures of neocortical neurons resulted in increased phosphorylation of AMPK, correlating with a robust induction of Bim expression that was evident within 8–24 h after AICAR addition (Fig. 4 E). A similar profile for AMPK activation and Bim expression was observed in CGNs treated with AICAR (Fig. S3 A). To investigate whether AMPK could modulate *bim* mRNA levels, we used luciferase reporter assays with a 0.8-kB fragment of the *bim* promoter (Sunters et al., 2003). Moreover, we examined whether overexpression of a constitutively active AMPK- $\alpha 1$  (CA-AMPK), rendered insensitive to phosphatase

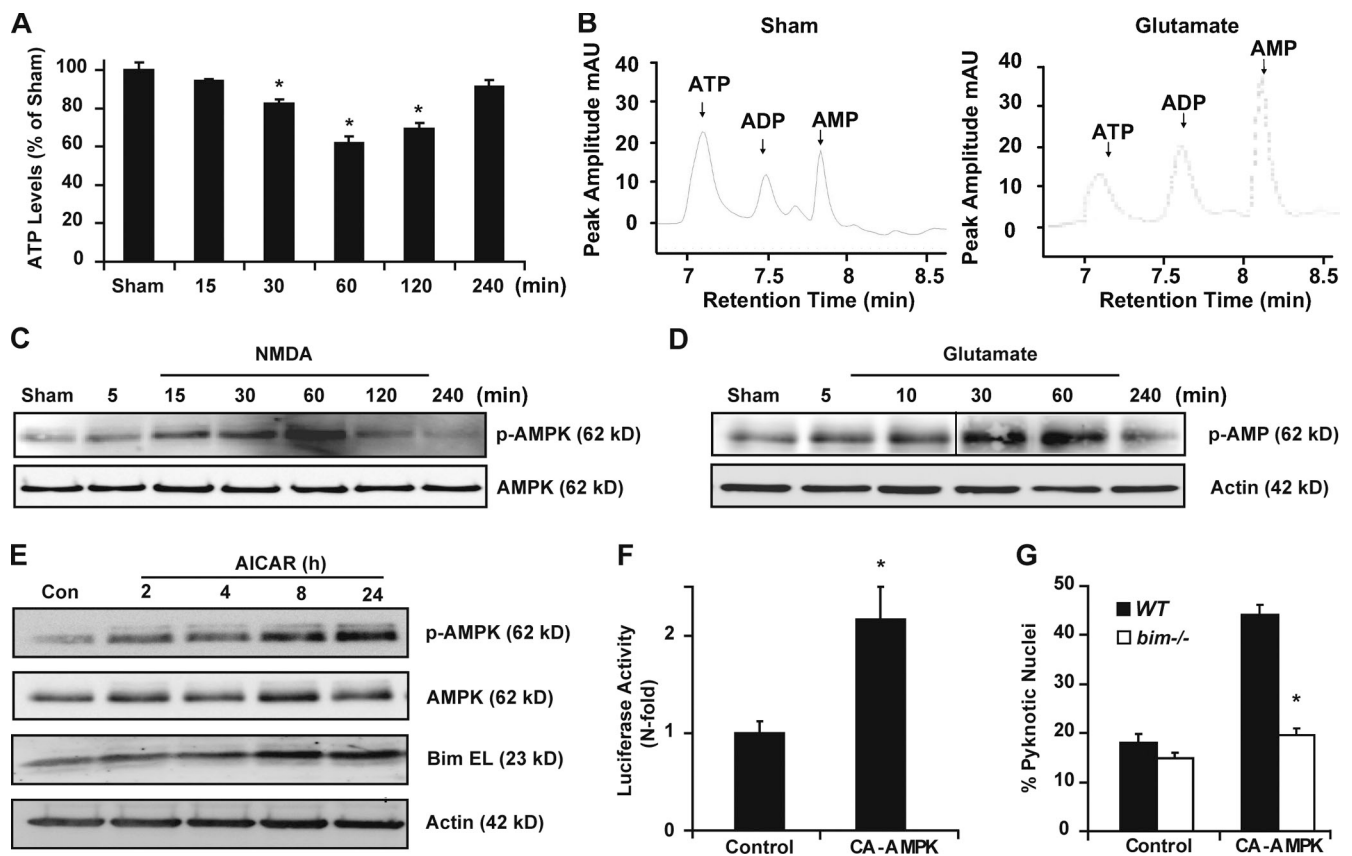


**Figure 4. AMPK is activated during excitotoxic apoptosis and is sufficient to induce *bim* expression.** (A) Neocortical neurons were treated with 100  $\mu$ M NMDA/10  $\mu$ M Gly or sham conditions for 5 min and allowed to recover for the indicated time periods. ATP levels were assessed relative to sham-treated controls. Data represent mean  $\pm$  SEM from  $n = 6$  cultures. This experiment was repeated twice with similar results. \*,  $P < 0.05$  compared with sham-treated cultures (ANOVA post-hoc Tukey). (B) Chromatograms of adenine nucleotides on reverse-phase column from sham (left) and 100  $\mu$ M glutamate/10  $\mu$ M Gly for 10 min (right). (C) Western blotting of phospho Thr172 AMPK levels in neocortical neurons at the indicated time periods after NMDA excitation. Total AMPK served as a loading control. Results are representative of at least two independent experiments. (D) Western blotting of phospho Thr172 AMPK levels in CGNs at the indicated time periods after glutamate excitation. Probing for  $\beta$ -actin served as loading control. Results are representative of at least two independent experiments. The vertical black line indicates that intervening lanes have been spliced out. (E) Neocortical neurons were treated with 2.5 mM AICAR for the indicated time periods. The levels of phospho Thr72 AMPK (p-AMPK), AMPK, Bim, and  $\beta$ -actin (loading control) were assessed by Western blotting. Results are representative of at least two independent experiments. (F) CGNs transfected with a vector containing a 0.8-kb fragment of the *bim* promoter and either a vector expressing CA-AMPK or control empty vector (control). Luminescence activity was normalized to the activity of the cotransfected TK-Renilla luciferase. Mean  $\pm$  SEM is shown. \*,  $P < 0.05$  compared with control vector (*t* test). (G) Neocortical neurons from WT and *bim*<sup>-/-</sup> mice were cotransfected with GFP and either a vector expressing CA-AMPK or a control empty vector, and the levels of pyknotic nuclei in 150–200 neurons per culture were assessed 24 h after transfection. Data represent mean  $\pm$  SEM from  $n = 4$  cultures per treatment. This experiment was repeated twice with similar results. \*,  $P < 0.05$  compared with CA-AMPK-transfected WT neurons (ANOVA post-hoc Tukey).

inactivation (Woods et al., 2000), could modulate *bim* promoter activity. Indeed, the expression of the CA-AMPK was associated with a significant increase in *bim* promoter activity (Fig. 4 F), indicating that AMPK can up-regulate *bim* mRNA levels. We next asked whether prolonged AMPK activation was sufficient to induce apoptosis in neurons, as reported in other cell types (Meisse et al., 2002; Kefas et al., 2003), and whether this was Bim dependent. Neocortical neurons from WT and *bim*<sup>-/-</sup> mice were cotransfected with vectors expressing CA-AMPK and GFP and analyzed for nuclear apoptosis after 24 h. Expression of CA-AMPK induced cell death within WT neocortical neurons, but neurons from *bim*<sup>-/-</sup> mice were highly resistant (Fig. 4 G). Likewise, CA-AMPK induced significant apoptosis in CGNs, and cotransfection with *bim* siRNA afforded protection compared with control siRNA (Fig. S3 B). Collectively, our data suggest that AMPK is activated during excitotoxic apoptosis and that prolonged activation is sufficient

for increased *bim* mRNA expression and to trigger a Bim-dependent cell death.

#### AMPK mediates excitotoxic apoptosis in a Bim-dependent manner

We noted that activation of AMPK with AICAR induced a significant activation of JNK (Fig. 5 A), which has previously been linked to excitotoxic apoptosis (Borsello et al., 2003; Chen et al., 2003), a finding reiterated in our excitotoxicity models (Fig. S4). Therefore, we addressed whether AMPK contributed to JNK activation during excitotoxic apoptosis. Using an siRNA construct targeting *AMPK- $\alpha$ 1/2* (Weisová et al., 2009), we down-regulated the expression of AMPK at the protein level (Fig. 5 B). Immunofluorescence analysis demonstrated increased nuclear accumulation of phosphorylated Ser63 c-Jun in control siRNA-transfected neurons after NMDA treatment (Fig. 5, C and D). In contrast, neurons expressing the *AMPK* siRNA

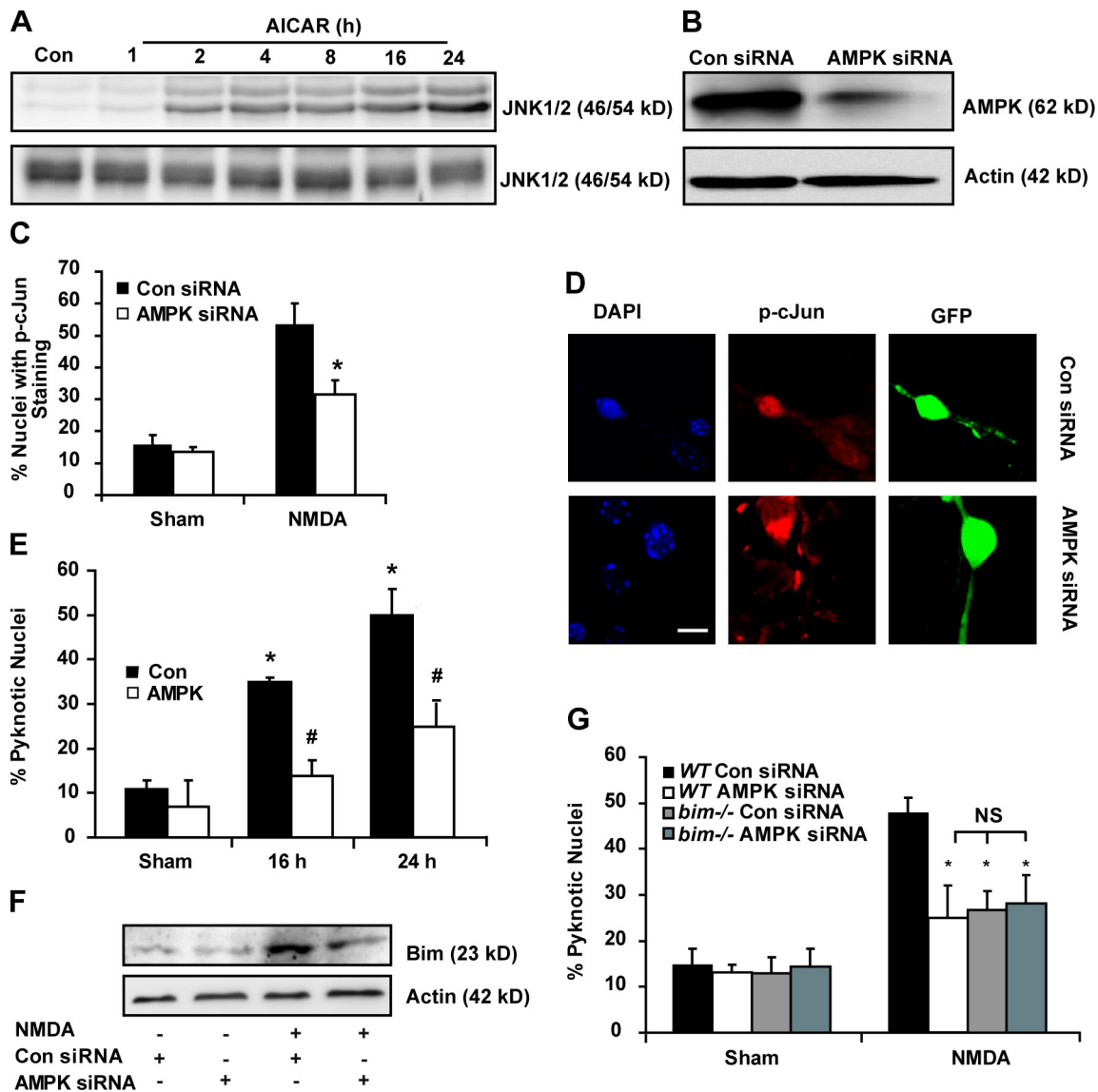


**Figure 5. AMPK mediates excitotoxic apoptosis in a Bim-dependent manner.** (A) Neocortical neurons were treated with 2.5 mM AICAR for the indicated time periods. Levels of p-JNK were assessed by Western blotting. Probing for total JNK served as a loading control. (B) Mouse neocortical neurons were transfected with a vector expressing either a control (Con) or AMPK siRNA sequence. AMPK levels were assessed 48 h after transfection by Western blotting. Probing for  $\beta$ -actin served as a loading control. (A and B) Results are representative of at least two independent experiments. (C) Neocortical neurons transfected with either control or AMPK siRNA cultured for 48 h and subsequently treated with 100  $\mu$ M NMDA/10  $\mu$ M Gly or sham conditions for 5 min and fixed after 16 h. The numbers of neurons with nuclear phospho Ser63 c-Jun (p-cJun) staining were quantified. Data represent mean  $\pm$  SEM from  $n = 3$  cultures. \*,  $P < 0.05$  compared with NMDA-treated control siRNA cultures (ANOVA post-hoc Tukey). (D) Representative images of neocortical neurons treated as described in C. Note the presence of nuclear phospho Ser63 c-Jun in control siRNA-transduced neurons but not in AMPK siRNA-transduced neurons. (E) Mouse cortical neurons were transfected with a vector expressing GFP and either an siRNA targeting AMPK or a control nontargeting siRNA and then cultured for 48 h. Neurons were subsequently treated with NMDA or sham and allowed to recover for 16–24 h before staining live with Hoechst. Pyknotic nuclei within the GFP-positive cells (250–300) were scored. Data represent mean  $\pm$  SEM from  $n = 4$  cultures. This experiment was repeated twice with similar results. \*,  $P < 0.05$  compared with sham-treated neurons; #,  $P < 0.05$  compared with control siRNA-transfected neurons at the same time point (ANOVA post-hoc Tukey). (F) Western blot demonstrating expression of Bim after NMDA treatment in neocortical neurons transfected either with control or AMPK siRNA. Probing for  $\beta$ -actin served as a loading control. (G) Neocortical neurons from WT and *bim*<sup>-/-</sup> mice were transfected with a vector expressing EGFP and either an siRNA targeting AMPK or a control nontargeting siRNA for 48 h. After NMDA treatment, pyknotic nuclei within the GFP-positive cells were scored (250–300 cells). Data represent mean  $\pm$  SEM from  $n = 4$  cultures. This experiment was repeated twice with similar results. \*,  $P < 0.05$  compared with NMDA treated with control siRNA (ANOVA post-hoc Tukey). Bar, 10  $\mu$ m.

had significantly reduced nuclear accumulation of phospho c-Jun. Furthermore, AMPK siRNA substantially inhibited excitotoxic apoptosis induced by NMDA (Fig. 5 E), and this was accompanied by reduced Bim induction after NMDA treatment (Fig. 5 F). Similarly, treatment with the pharmacological AMPK inhibitor compound C afforded protection against excitotoxic

apoptosis in neocortical neurons (Fig. S5). Finally, to confirm that AMPK triggers NMDA-mediated excitotoxicity through Bim, we assessed the impact of *ampk* knockdown on NMDA-induced apoptosis in *bim*<sup>-/-</sup> neurons. As with our previous experiments (Fig. 5 E), loss of Bim or knockdown of *ampk* significantly attenuated cell death within this paradigm

(Fig. 5 G). However, the knockdown of *ampk* expression in *bim*<sup>-/-</sup> neurons had no additive effect (Fig. 5 G) when compared with the control siRNA-transfected *bim*<sup>-/-</sup> neurons, suggesting that AMPK mediates excitotoxic apoptosis in a Bim-dependent manner.

## Discussion

A decrease in cellular bioenergetics as a consequence of ion homeostasis disruption has been previously almost exclusively linked to necrotic cell death (Ankarcrona et al., 1995; Bonfoco et al., 1995; Ward et al., 2000, 2007). This study now provides evidence that cellular ATP depletion is also required for the activation of proapoptotic signaling pathways during excitotoxic injury. We identified the proapoptotic BH3-only protein Bim as essential for the initiation of cell death within this paradigm. We also demonstrate that the energy sensor AMPK coupled energy depletion to *bim* mRNA induction and the subsequent activation of apoptosis in neurons.

Several studies have demonstrated that glutamate and NMDA receptor overactivation induce a rapid dysregulation of cellular ion homeostasis and an associated decrease in ATP levels, as neurons attempt to restore their ion homeostasis (Budd et al., 2000; Luetjens et al., 2000; Ward et al., 2000). AMPK is a Ser/Thr kinase that plays a fundamental role in the regulation of energy homeostasis, acting as an energy sensor to stresses that result in the depletion of ATP and increases in AMP. Increases in AMP levels such as those seen after NMDA treatment result in the allosteric activation of AMPK (Suter et al., 2006). However, several upstream kinases have been implicated in the phosphorylation and activation of AMPK, including the tumor suppressor LKB1 (Hawley et al., 2003) and Ca<sup>2+</sup>/calmodulin-dependent kinase kinase  $\beta$  (CaMKK- $\beta$ ; Hawley et al., 2005), which is activated via increases in intracellular Ca<sup>2+</sup>. Given the central role of Ca<sup>2+</sup> in mediating excitotoxic injury (Tymianski et al., 1993) and that CaMKK- $\beta$  is activated by increases in intracellular Ca<sup>2+</sup>, it is interesting to speculate that CaMKK- $\beta$  may play a functional role in the activation of AMPK during excitotoxicity.

AMPK has been implicated in the stimulation of catabolism, inhibition of fatty acid and cholesterol synthesis, and autophagy during energetic stress (Meley et al., 2006; Ronnett et al., 2009), all serving as attempts to provide energy substrates and enhance cellular ATP generation. Activation of glucose transporters is one of the key activities of AMPK in providing energy substrates to ATP-deprived cells (Hardie et al., 2006). As neurons rely significantly on glucose as their energy source, up-regulation of glucose transporters may represent a central step in AMPK action in neurons. Indeed, we previously demonstrated that glutamate excitation was associated with an AMPK-dependent increase in GLUT3 translocation and uptake of glucose into neurons (Weisová et al., 2009).

In this study, we provide evidence that activation of AMPK is also required to induce excitotoxic apoptosis and show that prolonged AMPK activation can be sufficient to trigger neuronal apoptosis. Multiple studies have demonstrated that prolonged AMPK activation with AICAR can be

toxic to nonneuronal cells (Meisse et al., 2002; Kefas et al., 2003). Therefore, AMPK can be added to the growing list of kinases and transcription factors that have dual functions in the regulation of cell survival or cell death depending on the type of stress and type of cell, as reported for JNK, Foxo3a, and NF- $\kappa$ B (nuclear factor  $\kappa$ B; O'Neill and Kaltschmidt, 1997; Biswas et al., 2007; Mojsilovic-Petrovic et al., 2009). A key task for future studies will be to elucidate the mechanisms of cell fate switches by these signaling molecules. Signal intensity and subcellular location as well as transient (or oscillatory) versus persistent activation kinetics may critically determine cell fate. In this context, a transient activation of AMPK in neurons before glucose deprivation has been shown to be neuroprotective (Culmsee et al., 2001; Weisová et al., 2009), whereas inhibition of AMPK activity with compound C administered at the onset of cerebral ischemia or genetic deletion of AMPK- $\alpha$ 2 provided significant protection after middle cerebral artery occlusion in vivo (McCullough et al., 2005; Li et al., 2007). AMPK has been shown to influence several long-term processes and cell fate decisions in addition to the acute regulation of cellular bioenergetics such as cell cycle arrest and cell polarity (Gwinn et al., 2008). In this study, we demonstrate that prolonged AMPK activation is also directly associated with the transcriptional induction of the BH3-only protein Bim and activation of the Bcl-2-regulated apoptotic pathway.

Several different factors have been implicated in the regulation of the *bim* gene in neurons, including JNK/c-Jun (Harris and Johnson, 2001; Whitfield et al., 2001), Foxo3a (Sunter et al., 2003; Biswas et al., 2007), and C-myb (Biswas et al., 2007). Previous studies have demonstrated the activation of JNK during excitotoxic injury and the neuroprotection achieved by JNK inhibition in these scenarios (Borsello et al., 2003; Chen et al., 2003; Centeno et al., 2007). Indeed, AMPK activation has also been linked to subsequent downstream JNK activity during apoptosis (Meisse et al., 2002; Kefas et al., 2003; Lee et al., 2008). However, it should be noted that the regulation of *bim* expression is highly complex (Biswas et al., 2007), and other pathways independent of JNK signaling may well be required for Bim-dependent excitotoxic apoptosis. A recent study has shown that AMPK can phosphorylate and enhance the transcriptional activity of Foxo3a (Greer et al., 2007). In addition, given that AMPK can down-regulate mTOR (mammalian target of rapamycin) signaling, this may in turn result in decreased Akt phosphorylation, nuclear translocation of Foxo3a, and induction of *bim*. Although we could demonstrate a role for AMPK in the regulation of Bim induction, it remains plausible that NMDA-mediated excitotoxic injury may also have an impact on JNK, Foxo3a, or other cellular signaling pathways independent of AMPK activity to regulate Bim expression. Indeed, it remains plausible that the activation of AMPK by itself may not be sufficient for Bim induction in certain cell types and/or settings, and the AMPK-mediated regulation of Bim expression may be dependent on the manner of AMPK activation.

Our data also suggest that *bim* expression is central to DCD and the late collapse of the  $\Delta\psi_m$ , which are cellular events not previously linked to gene induction after an excitotoxic stimulus. Indeed, the time frame of *bim* mRNA induction preceded the



delayed  $\Delta\psi_m$  depolarization and DCD, with the frequency of both of these events diminished in *bim*-deficient neurons. We and others provided evidence for the mitochondrial release of cytochrome *c* and AIF during excitotoxic apoptosis (Luetjens et al., 2000; Wang et al., 2004). Cytochrome *c* release in mature neurons may not be sufficient to cause a large extent of executioner caspase activity caused by increased XIAP (X-linked inhibitor of apoptosis protein) levels, reduced expression of APAF-1, and calpain-mediated degradation of caspases (Lankiewicz et al., 2000; Yakovlev et al., 2001; Potts et al., 2003). AIF plays a central role in caspase-independent excitotoxic apoptosis, where it substitutes for caspases to induce nuclear condensation (Wang et al., 2004; Cheung et al., 2005).

In this study, we demonstrate a requirement for Bim in excitotoxic apoptosis. This form of cell death contrasts with excitotoxic necrosis, in which  $\Delta\psi_m$  does not recover and cell lysis occurs in the absence of nuclear condensation (Ankarcrona et al., 1995; Ward et al., 2006). Nevertheless, we cannot exclude that other pathways were activated that mediate alternative or intermediate cell death types or work in parallel to Bim-dependent apoptosis. These might include the  $Ca^{2+}$ -mediated opening of the mitochondrial permeability transition pore (PTP; Baines et al., 2005), the activation of calpains (Bano et al., 2005), and the activation of PARP-1 (Mandir et al., 2000). Of particular note, the activation of PARP-1 during excitotoxicity results in the depletion of intracellular pools of  $NAD^+$ , which the enzyme uses as a substrate (Liu et al., 2008). This in turn results in a depletion of ATP levels as  $NAD^+$  synthetase is activated to synthesize  $NAD^+$  and a reduced concentration of  $NAD^+$  is available for reduction to the high energy substrate NADH. This may create a positive feed-forward signal for AMPK activation and consequent *bim* induction. Indeed  $NAD^+$  supplementation has been shown to protect neurons from excitotoxic injury (Liu et al., 2008). Similarly, PTP opening depletes mitochondrial ATP production, and the activation of calpains can further increase neuronal  $Ca^{2+}$  overloading (Bano et al., 2005), thereby increasing the ATP demand. However, as PARP-1 activation, PTP opening, and calpain activation also occur physiologically, it is reasonable to assume that AMPK-dependent *bim* gene activation represents a key gateway for the activation of excitotoxic apoptosis.

In conclusion, we demonstrate that depletion of cellular ATP is a key signaling switch in the activation of proapoptotic signaling pathways during excitotoxic injury. This process requires AMPK and the activation of the proapoptotic BH3-only protein Bim. These findings have the potential to be translated to numerous pathophysiological settings in which moderate to severe energy depletion may lead to the execution of apoptosis.

## Materials and methods

### Preparation of rat CGNs and mouse neocortical neurons

Mouse neocortex or rat (Sprague-Dawley) cerebellum was isolated from embryonic day 16 or postnatal day 7 pups, respectively. The isolated tissue was then transferred to dissection medium on ice (PBS with 0.25% glucose and 0.3% BSA). The tissue was incubated with 0.25% trypsin-EDTA at 37°C for 15 min. After the incubation, the trypsinization was

stopped by the addition of medium containing sera. The neurons were then dissociated by gentle pipetting, and after centrifugation (1,500 rpm for 3 min) the medium containing trypsin was aspirated. Neocortical neurons were resuspended in fresh plating medium (MEM containing 5% fetal calf serum, 5% horse serum, 100 U/ml penicillin/streptomycin, 0.5 mM L-Gln, and 0.6% D-glucose), whereas CGNs were resuspended in MEM containing 10% fetal calf serum, 100 U/ml penicillin/streptomycin, 0.5 mM L-Gln, 4 mM KCl, and 0.6% D-glucose. Cells were plated at  $2 \times 10^5$  cells/cm<sup>2</sup> on poly-l-lys-coated plates and incubated at 37°C, 5% CO<sub>2</sub>. The plating medium was exchanged for feeding medium the following day. Neurobasal medium-embryonic containing 100 U/ml penicillin/streptomycin, 2% B27, and 0.5 mM L-Gln and 600 nM cytosine arabinofuranoside for neocortical neurons and 1:1 plating medium/feeding medium (plating medium minus L-Gln) and 10  $\mu$ M cytosine arabinofuranoside for CGNs. One third of the medium was exchanged for fresh medium every 2–3 d until day in vitro (DIV) 6. Experiments were performed until DIV 9.

### OHSCs

OHSCs were prepared and cultured according to the modified procedure (Kristensen et al., 2001). The brain from postnatal day 10 mouse pups was isolated and transferred to dissection medium containing HBSS (Invitrogen), 20 mM Hepes, 100 U/ml penicillin, 100  $\mu$ g/ml streptomycin, and 0.65% glucose. Isolated hippocampi were placed on a McIlwain tissue chopper (Mickle Laboratory Engineering) and cut into 450- $\mu$ m-thick sections. The slices were then transferred onto the porous (0.4  $\mu$ m) membrane of millicell inserts (Millipore). The inserts were placed in 24-well tissue culture plates with 250  $\mu$ l of culture medium consisting of MEM (Sigma-Aldrich) supplemented with 25% horse serum, 4 mM L-Gln, 6 mg/ml D-glucose, 2% B27, 50 U/ml penicillin G, and 50  $\mu$ g/ml streptomycin (Sigma-Aldrich). The slices were maintained in a humidified incubator with 5% CO<sub>2</sub> at 35°C with media changes every other day. All experiments were performed at DIV 10.

### Confocal microscopy

Primary neocortical neurons or CGNs were loaded with 3  $\mu$ M Fluo-4 AM and 20 nM TMRM in experimental buffer (120 mM NaCl, 3.5 mM KCl, 0.4 mM KH<sub>2</sub>PO<sub>4</sub>, 20 mM Hepes, 5 mM NaHCO<sub>3</sub>, 1.2 mM Na<sub>2</sub>SO<sub>4</sub>, 1.2 mM CaCl<sub>2</sub>, 1.2 mM MgCl<sub>2</sub>, and 15 mM glucose, pH 7.4) for 30 min at 37°C. The buffer was then exchanged for buffer without Fluo-4 AM and placed on the stage of a confocal microscope (LSM 510 Meta; Carl Zeiss, Inc.) with a 63 $\times$  NA 1.4 differential interference contrast objective with a thermostatically regulated chamber maintained at 37°C. 10  $\mu$ M MK-801 was added to block open channel NMDA receptors after receptor stimulation. Fluo-4 AM was excited at 488 nm with the emission collected by a 505–550-nm filter, TMRM was excited at 543 nm, and the emission was collected with by a 560-nm-long pass filter. Images were captured at 15-s intervals during excitation and every 5 min for the rest of the experiment. The resulting images were processed and analyzed using MetaMorph software (7.0r1-4; MDS Analytical Technologies).

### Real-time qPCR

Total RNA was extracted using the RNeasy mini kit (QIAGEN). First strand cDNA synthesis was performed using 2  $\mu$ g of total RNA as template and reverse transcribed using Superscript II (Invitrogen) primed with 50 pmol of random hexamers. Real-time qPCR was performed using the Light-Cycler 2.0 (Roche) and the QuantiTech SYBR green PCR kit (QIAGEN). Sense and antisense primers were as follows: 5'-CCAGCTGACTGCCCT-GCTA-3' and 5'-AGCAACTTCACCTGCTGTGC-3' for *bim*; 5'-ACGA-C AAGGCCATGCTGATA-3' and 5'-AGGCACCTCAGTCCATCTC-3' for *bid*; 5'-GAGACGCTGCTCCTGGAGTCA-3' and 5'-GGCCTGTCTT-CCTGGCTA-3' for *bmf*; 5'-ATGGACTCAGCATCGGAAGG-3' and 5'-TGGCTCATTGCTCTTCACG-3' for *puma*; and 5'-AGCCATCCAG-GCTGTGTGTG-3' and 5'-CAGCTGTGGTGGTGAAGCTG-3' for *actin*. The data were analyzed using the LightCycler software 4.0 (Roche) with all samples normalized to  $\beta$ -actin.

### Western blotting

Preparation of cell lysates and Western blotting were performed as described previously (Weisová et al., 2009). Blots were probed with either rabbit polyclonal antibodies to Bim (StressGen) diluted 1:1,000, phospho (Thr172) AMPK antibody (Cell Signaling Technology) diluted 1:1,000, total AMPK (Cell Signaling Technology) diluted 1:1,000, phospho (Thr183/Thr185) JNK (Cell Signaling Technology) diluted 1:1,000, total JNK (Cell Signaling Technology) diluted 1:1,000, PUMA-NT (ProSci) diluted 1:500, an anti-goat Bid antibody (R&D Systems) diluted 1:1,000, or a mouse monoclonal anti- $\beta$ -actin antibody (clone DM 1A; Sigma-Aldrich),

diluted 1:5,000. Horseradish peroxidase-conjugated secondary antibodies diluted 1:10,000 (Thermo Fisher Scientific) were detected using SuperSignal West Pico Chemiluminescent Substrate (Thermo Fisher Scientific) and imaged using an imaging system (LAS-3000; Fujifilm).

#### Determination of neuronal injury: Hoechst and PI staining of nuclear chromatin

Neocortical neurons and CGNs were stained live with 1  $\mu\text{g}/\text{ml}$  Hoechst 33258 in medium. Nuclear morphology was assessed using an inverted microscope (Eclipse TE 300; Nikon) with a 20 $\times$  NA 0.43 phase contrast objective using the appropriate filter set for Hoechst and a charge-coupled device camera (SPOT RT SE 6; Diagnostic Instruments, Inc.) and Wasabi software (Hamamatsu Photonics). For each time point, images of apoptotic morphology were captured in three subfields and repeated in triplicate. Resultant images were processed using ImageJ (Micron-Optica; National Institutes of Health). Condensed nuclei were scored as pyknotic nuclei and expressed as a percentage of the total population. For the determination of neuronal injury in OHSCs, slices were stained live with 5  $\mu\text{g}/\text{ml}$  PI for 15 min before image acquisition. Images were captured before and after treatment using the TE 300 microscope with a 4 $\times$  NA 0.13 phase objective and captured using a SPOT RT SE 6 charge-coupled device and Wasabi software and the appropriate filter set for PI. Illumination and exposure (camera gain and exposure time) were kept constant throughout each series of recordings and between experiments. Images were processed using ImageJ. A suitable region of interest was selected, and increase in mean fluorescent intensity was determined. Background intensity was accounted for, and neuronal injury was expressed as a percentage of total injury (1 mM NMDA for 1 h and sham conditions with 10  $\mu\text{M}$  MK-801 was used to assess the fluorescent dynamic range). All experiments were performed at least three times with independent cultures.

#### Plasmids, transfections, and siRNA

The plasmid encoding the CA-AMPK (Woods et al., 2000) was a gift from D. Carling (Imperial College London, London, England, UK). Neocortical neurons were transfected at DIV 5 using Lipofectamine 2000 (Invitrogen). CGNs were transfected using  $\text{Ca}^{2+}$  phosphate as previously described (Weisová et al., 2009). For inhibition of AMPK, cells were transfected with a vector expressing either an siRNA targeting AMPK- $\alpha 1/\alpha 2$  or a control sequence as previously described (Weisová et al., 2009). Silencing of Bim expression was performed using siRNA duplexes purchased from Sigma-Aldrich. Sequences were as follows: Bim sense, 5'-CGGGACAG-CAGAGAAGAU(CdTdT)-3'; Bim antisense, 5'-GAUCUUCUCUGCUGUC-CCG(dTdT)-3'; control sense, 5'-ACUUAACCGGCAUACCGGC(dTdT)-3'; and control antisense, 5'-GCCGGUAUGCCGGUUAAGU(dTdT)-3'.

#### Luciferase assays

CGNs were transfected with a reporter construct containing 0.8 kb of the Bim promoter construct (gift from E. Lam, Imperial College London; Sinters et al., 2003) using the transfection agent Neurofect (Genlantis) in neurobasal medium supplemented with 10% B27, 25 mM KCl, and 2 mM Glu. For luciferase assays, neurons were lysed in passive lysis buffer, and luciferase activity was analyzed using a luminometer and dual luciferase assay kit (Promega) according to the manufacturer's instructions. Transfections were performed in triplicate dishes, and luciferase counts (relative luminescence units) were normalized using TK-Renilla luciferase cotransfection.

#### ATP assay

After appropriate treatments, neurons were lysed using a hypotonic lysis buffer (Tris-acetate buffer, pH 7.75). ATP measurements were performed using the ENLITEN ATP Assay System Bioluminescence Detection kit (Promega) according to the manufacturer's instructions, and the resultant luminescence was monitored using a luminometer (Centro LB960; Berthold). The amount of ATP was determined by a standard concentration curve, and ATP content values were corrected for protein concentration and normalized to sham-treated samples.

#### HPLC measurement of intracellular AMP and ATP levels

ATP and AMP levels were monitored by means of HPLC analysis. Neurons were lysed in 0.5 M KOH and adjusted to pH 6.5 by the addition of 1 M  $\text{KH}_2\text{PO}_4$ . HPLC analysis of AMP and ATP peaks was performed as previously described (Weisová et al., 2009).

#### Immunofluorescence analysis

Cells were fixed with 4% paraformaldehyde for 20 min, permeabilized in PBS containing 1% Triton X-100, washed three times with PBS, and blocked for 1 h in 5% goat serum in PBS. The primary antibodies used were either

a rabbit polyclonal anti-AIF antibody (Suter et al., 2000) diluted 1:500 (gift from M. Jäättelä, Danish Cancer Society, Copenhagen, Denmark) or a rabbit polyclonal anti-phospho (Ser63) c-Jun antibody (Cell Signaling Technology) diluted 1:250. Primary antibodies were detected by incubation for 2 h at room temperature in a 1:500 dilution of either FITC- or rhodamine-conjugated goat anti-rabbit secondary antibody (Jackson ImmunoResearch Laboratories, Inc.).

#### Gene-targeted mice

The generation and genotyping of *puma*<sup>-/-</sup>, *bim*<sup>-/-</sup>, and *bid*<sup>-/-</sup> mice have previously been described (Bouillet et al., 1999; Villunger et al., 2003; Kaufmann et al., 2007). The *puma*<sup>-/-</sup> and *bid*<sup>-/-</sup> mice were generated on an inbred C57BL/6 background, using C57BL/6-derived embryonic stem cells. The *bim*<sup>-/-</sup> mice were originally generated on a mixed C57BL/6  $\times$  129SV genetic background, using 129SV-derived embryonic stem cells, but had been backcrossed for >12 generations onto the C57BL/6 background.

#### Statistical analysis

Data are presented as means  $\pm$  SEM. For statistical comparison, one-way analysis of variance (ANOVA) followed by Tukey's test was used. P-values <0.05 were considered to be statistically significant.

#### Online supplemental material

Fig. S1 shows the quantification of neuronal cell death after NMDA treatment. Fig. S2 shows the up-regulation of Bim in OHSCs subjected to NMDA-induced excitotoxic injury. Fig. S3 shows that AMPK activation triggers Bim-dependent cell death in CGNs. Fig. S4 shows that JNK inhibition protects against excitotoxic apoptosis. Fig. S5 shows that compound C reduces NMDA-induced excitotoxic injury. Online supplemental material is available at <http://www.jcb.org/cgi/content/full/jcb.200909166/DC1>.

We are grateful to Prof. David Carling for the gift of the CA-AMPK plasmid, Prof. Eric Lam for the Bim promoter plasmid, and Prof. Marja Jäättelä for the AIF antibody. We thank David Kennedy for help with HPLC experiments and Ina Woods, Simone Poeschel, and Sarah Cannon for excellent technical assistance.

This study was supported by grants from Science Foundation Ireland (08/IN1/1949) and the Health Research Board (RP/2006/333) to J.H.M. Prehn as well as the National Health and Medical Research Council (program #461221) to A. Strasser. L.P. Tuffy is a recipient of an Irish Research Council for Science, Engineering, and Technology scholarship (325/2005), and D. Dávila holds a Marie Curie Intra-European Fellowship for Career Development (PIEF-GA-2009-237765).

Submitted: 28 September 2009

Accepted: 8 March 2010

## References

- Ankarcrona, M., J.M. Dypbukt, E. Bonfoco, B. Zhivotovsky, S. Orrenius, S.A. Lipton, and P. Nicotera. 1995. Glutamate-induced neuronal death: a succession of necrosis or apoptosis depending on mitochondrial function. *Neuron*. 15:961–973. doi:10.1016/0896-6273(95)90186-8
- Baines, C.P., R.A. Kaiser, N.H. Purcell, N.S. Blair, H. Osinska, M.A. Hambleton, E.W. Brunskill, M.R. Sayen, R.A. Gottlieb, G.W. Dorn, et al. 2005. Loss of cyclophilin D reveals a critical role for mitochondrial permeability transition in cell death. *Nature*. 434:658–662. doi:10.1038/nature03434
- Bano, D., K.W. Young, C.J. Guerin, R. Lefevre, N.J. Rothwell, L. Naldini, R. Rizzuto, E. Carafoli, and P. Nicotera. 2005. Cleavage of the plasma membrane  $\text{Na}^+/\text{Ca}^{2+}$  exchanger in excitotoxicity. *Cell*. 120:275–285. doi:10.1016/j.cell.2004.11.049
- Biswas, S.C., Y. Shi, A. Sproul, and L.A. Greene. 2007. Pro-apoptotic Bim induction in response to nerve growth factor deprivation requires simultaneous activation of three different death signaling pathways. *J. Biol. Chem.* 282:29368–29374. doi:10.1074/jbc.M702634200
- Bonfoco, E., D. Krainc, M. Ankarcrona, P. Nicotera, and S.A. Lipton. 1995. Apoptosis and necrosis: two distinct events induced, respectively, by mild and intense insults with N-methyl-D-aspartate or nitric oxide/superoxide in cortical cell cultures. *Proc. Natl. Acad. Sci. USA*. 92:7162–7166. doi:10.1073/pnas.92.16.7162
- Borsello, T., P.G.H. Clarke, L. Hirt, A. Vercelli, M. Repici, D.F. Schorderet, J. Bogousslavsky, and C. Bonny. 2003. A peptide inhibitor of c-Jun N-terminal kinase protects against excitotoxicity and cerebral ischemia. *Nat. Med.* 9:1180–1186. doi:10.1038/nm911

- Bouillet, P., D. Metcalf, D.C. Huang, D.M. Tarlinton, T.W. Kay, F. Köntgen, J.M. Adams, and A. Strasser. 1999. Proapoptotic Bcl-2 relative Bim required for certain apoptotic responses, leukocyte homeostasis, and to preclude autoimmunity. *Science*. 286:1735–1738. doi:10.1126/science.286.5445.1735
- Brines, M.L., and R.J. Robbins. 1992. Inhibition of alpha 2/alpha 3 sodium pump isoforms potentiates glutamate neurotoxicity. *Brain Res.* 591:94–102. doi:10.1016/0006-8993(92)90982-F
- Budd, S.L., L. Tennen, T. Lishnak, and S.A. Lipton. 2000. Mitochondrial and extramitochondrial apoptotic signaling pathways in cerebrocortical neurons. *Proc. Natl. Acad. Sci. USA.* 97:6161–6166. doi:10.1073/pnas.100121097
- Centeno, C., M. Repici, J.Y. Chatton, B.M. Riederer, C. Bonny, P. Nicod, M. Price, P.G.H. Clarke, S. Papa, G. Franzoso, and T. Borsello. 2007. Role of the JNK pathway in NMDA-mediated excitotoxicity of cortical neurons. *Cell Death Differ.* 14:240–253. doi:10.1038/sj.cdd.4401988
- Chen, R.W., Z.H. Qin, M. Ren, H. Kanai, E. Chalecka-Franaszek, P. Leeds, and D.M. Chuang. 2003. Regulation of c-Jun N-terminal kinase, p38 kinase and AP-1 DNA binding in cultured brain neurons: roles in glutamate excitotoxicity and lithium neuroprotection. *J. Neurochem.* 84:566–575. doi:10.1046/j.1471-4159.2003.01548.x
- Cheung, E.C.C., L. Melanson-Drapeau, S.P. Cregan, J.L. Vanderluit, K.L. Ferguson, W.C. McIntosh, D.S. Park, S.A.L. Bennett, and R.S. Slack. 2005. Apoptosis-inducing factor is a key factor in neuronal cell death propagated by BAX-dependent and BAX-independent mechanisms. *J. Neurosci.* 25:1324–1334. doi:10.1523/JNEUROSCI.4261-04.2005
- Choi, D.W. 1987. Ionic dependence of glutamate neurotoxicity. *J. Neurosci.* 7:369–379.
- Choi, D.W., and S.M. Rothman. 1990. The role of glutamate neurotoxicity in hypoxic-ischemic neuronal death. *Annu. Rev. Neurosci.* 13:171–182. doi:10.1146/annurev.ne.13.030190.001131
- Choi, D.W., M. Maulucci-Gedde, and A.R. Kriegstein. 1987. Glutamate neurotoxicity in cortical cell culture. *J. Neurosci.* 7:357–368.
- Culmsee, C., J. Monnig, B.E. Kemp, and M.P. Mattson. 2001. AMP-activated protein kinase is highly expressed in neurons in the developing rat brain and promotes neuronal survival following glucose deprivation. *J. Mol. Neurosci.* 17:45–58. doi:10.1385/JMN:17:1:45
- Dawson, V.L., T.M. Dawson, E.D. London, D.S. Bredt, and S.H. Snyder. 1991. Nitric oxide mediates glutamate neurotoxicity in primary cortical cultures. *Proc. Natl. Acad. Sci. USA.* 88:6368–6371. doi:10.1073/pnas.88.14.6368
- Dietz, G.P., B. Dietz, and M. Bähr. 2007. Bcl-xL protects cerebellar granule neurons against the late phase, but not against the early phase of glutamate-induced cell death. *Brain Res.* 1164:136–141. doi:10.1016/j.brainres.2007.06.025
- Greer, E.L., P.R. Oskoui, M.R. Banko, J.M. Maniar, M.P. Gygi, S.P. Gygi, and A. Brunet. 2007. The energy sensor AMP-activated protein kinase directly regulates the mammalian FOXO3 transcription factor. *J. Biol. Chem.* 282:30107–30119. doi:10.1074/jbc.M705325200
- Gwinn, D.M., D.B. Shackelford, D.F. Egan, M.M. Mihaylova, A. Mery, D.S. Vasquez, B.E. Turk, and R.J. Shaw. 2008. AMPK phosphorylation of raptor mediates a metabolic checkpoint. *Mol. Cell.* 30:214–226. doi:10.1016/j.molcel.2008.03.003
- Hardie, D.G., S.A. Hawley, and J.W. Scott. 2006. AMP-activated protein kinase—development of the energy sensor concept. *J. Physiol.* 574:7–15. doi:10.1113/jphysiol.2006.108944
- Harris, C.A., and E.M. Johnson Jr. 2001. BH3-only Bcl-2 family members are coordinately regulated by the JNK pathway and require Bax to induce apoptosis in neurons. *J. Biol. Chem.* 276:37754–37760.
- Hawley, S.A., J. Boudeau, J.L. Reid, K.J. Mustard, L. Udd, T.P. Mäkelä, D.R. Alessi, and D.G. Hardie. 2003. Complexes between the LKB1 tumor suppressor, STRAD alpha/beta and MO25 alpha/beta are upstream kinases in the AMP-activated protein kinase cascade. *J. Biol.* 2:28. doi:10.1186/1475-4924-2-28
- Hawley, S.A., D.A. Pan, K.J. Mustard, L. Ross, J. Bain, A.M. Edelman, B.G. Frenguelli, and D.G. Hardie. 2005. Calmodulin-dependent protein kinase-beta is an alternative upstream kinase for AMP-activated protein kinase. *Cell Metab.* 2:9–19. doi:10.1016/j.cmet.2005.05.009
- Kaufmann, T., L. Tai, P.G. Ekert, D.C. Huang, F. Norris, R.K. Lindemann, R.W. Johnstone, V.M. Dixit, and A. Strasser. 2007. The BH3-only protein bid is dispensable for DNA damage- and replicative stress-induced apoptosis or cell-cycle arrest. *Cell.* 129:423–433. doi:10.1016/j.cell.2007.03.017
- Kefas, B.A., Y. Cai, Z. Ling, H. Heimberg, L. Hue, D. Pipeleers, and M. Van de Castele. 2003. AMP-activated protein kinase can induce apoptosis of insulin-producing MIN6 cells through stimulation of c-Jun-N-terminal kinase. *J. Mol. Endocrinol.* 30:151–161. doi:10.1677/jme.0.0300151
- Kristensen, B.W., J. Norberg, and J. Zimmer. 2001. Comparison of excitotoxic profiles of ATPA, AMPA, KA and NMDA in organotypic hippocampal slice cultures. *Brain Res.* 917:21–44. doi:10.1016/S0006-8993(01)02900-6
- Lankiewicz, S., C. Marc Luetjens, N. Truc Bui, A.J. Krohn, M. Poppe, G.M. Cole, T.C. Saido, and J.H. Prehn. 2000. Activation of calpain I converts excitotoxic neuron death into a caspase-independent cell death. *J. Biol. Chem.* 275:17064–17071. doi:10.1074/jbc.275.22.17064
- Lee, Y.M., K.-O. Uhm, E.S. Lee, J. Kwon, S.H. Park, and H.S. Kim. 2008. AM251 suppresses the viability of HepG2 cells through the AMPK (AMP-activated protein kinase)-JNK (c-Jun N-terminal kinase)-ATF3 (activating transcription factor 3) pathway. *Biochem. Biophys. Res. Commun.* 370:641–645. doi:10.1016/j.bbrc.2008.04.003
- Li, J., Z. Zeng, B. Viollet, G.V. Ronnett, and L.D. McCullough. 2007. Neuroprotective effects of adenosine monophosphate-activated protein kinase inhibition and gene deletion in stroke. *Stroke.* 38:2992–2999. doi:10.1161/STROKEAHA.107.490904
- Liu, D., M. Pitta, and M.P. Mattson. 2008. Preventing NAD(+) depletion protects neurons against excitotoxicity: bioenergetic effects of mild mitochondrial uncoupling and caloric restriction. *Ann. N. Y. Acad. Sci.* 1147:275–282.
- Luetjens, C.M., N.T. Bui, B. Sengpiel, G. Münstermann, M. Poppe, A.J. Krohn, E. Bauerbach, J. Kriegstein, and J.H.M. Prehn. 2000. Delayed mitochondrial dysfunction in excitotoxic neuron death: cytochrome c release and a secondary increase in superoxide production. *J. Neurosci.* 20:5715–5723.
- Mandir, A.S., M.F. Poiras, A.R. Berliner, W.J. Herring, D.B. Guastella, A. Feldman, G.G. Poirier, Z.Q. Wang, T.M. Dawson, and V.L. Dawson. 2000. NMDA but not non-NMDA excitotoxicity is mediated by Poly(ADP-ribose) polymerase. *J. Neurosci.* 20:8005–8011.
- McCullough, L.D., Z. Zeng, H. Li, L.E. Landree, J. McFadden, and G.V. Ronnett. 2005. Pharmacological inhibition of AMP-activated protein kinase provides neuroprotection in stroke. *J. Biol. Chem.* 280:20493–20502. doi:10.1074/jbc.M409985200
- Meisse, D., M. Van de Castele, C. Beauloye, I. Hainault, B.A. Kefas, M.H. Rider, F. Fougelle, and L. Hue. 2002. Sustained activation of AMP-activated protein kinase induces c-Jun N-terminal kinase activation and apoptosis in liver cells. *FEBS Lett.* 526:38–42. doi:10.1016/S0014-5793(02)03110-1
- Meley, D., C. Bauvy, J.H.P.M. Houben-Weerts, P.F. Dubbelhuis, M.T.J. Helmond, P. Codogno, and A.J. Meijer. 2006. AMP-activated protein kinase and the regulation of autophagic proteolysis. *J. Biol. Chem.* 281:34870–34879. doi:10.1074/jbc.M605488200
- Mironov, S.L. 1995. Plasmalemmal and intracellular Ca<sup>2+</sup> pumps as main determinants of slow Ca<sup>2+</sup> buffering in rat hippocampal neurones. *Neuropharmacology.* 34:1123–1132. doi:10.1016/0028-3908(95)00080-P
- Mojsilovic-Petrovic, J., N. Nedelsky, M. Boccitto, I. Mano, S.N. Georgiades, W. Zhou, Y. Liu, R.L. Neve, J.P. Taylor, M. Driscoll, et al. 2009. FOXO3a is broadly neuroprotective in vitro and in vivo against insults implicated in motor neuron diseases. *J. Neurosci.* 29:8236–8247. doi:10.1523/JNEUROSCI.1805-09.2009
- O'Neill, L.A., and C. Kalschmidt. 1997. NF-kappa B: a crucial transcription factor for glial and neuronal cell function. *Trends Neurosci.* 20:252–258. doi:10.1016/S0166-2236(96)01035-1
- Potts, P.R., S. Singh, M. Knezek, C.B. Thompson, and M. Deshmukh. 2003. Critical function of endogenous XIAP in regulating caspase activation during sympathetic neuronal apoptosis. *J. Cell Biol.* 163:789–799. doi:10.1083/jcb.200307130
- Ronnett, G.V., S. Ramamurthy, A.M. Kleman, L.E. Landree, and S. Aja. 2009. AMPK in the brain: its roles in energy balance and neuroprotection. *J. Neurochem.* 109:17–23. doi:10.1111/j.1471-4159.2009.05916.x
- Rothstein, J.D., G. Tsai, R.W. Kuncl, L. Clawson, D.R. Cornblath, D.B. Drachman, A. Pestronk, B.L. Stauch, and J.T. Coyle. 1990. Abnormal excitatory amino acid metabolism in amyotrophic lateral sclerosis. *Ann. Neurol.* 28:18–25. doi:10.1002/ana.410280106
- Ruiz, F., G. Alvarez, R. Pereira, M. Hernández, M. Villalba, F. Cruz, S. Cerdán, E. Bógón, and J. Sastrústegui. 1998. Protection by pyruvate and malate against glutamate-mediated neurotoxicity. *Neuroreport.* 9:1277–1282.
- Semenova, M.M., A.M. Mäki-Hokkonen, J. Cao, V. Komarovski, K.M. Forsberg, M. Koistinaho, E.T. Coffey, and M.J. Courtney. 2007. Rho mediates calcium-dependent activation of p38alpha and subsequent excitotoxic cell death. *Nat. Neurosci.* 10:436–443.
- Sunters, A., S. Fernández de Mattos, M. Stahl, J.J. Brosens, G. Zoumpoulidou, C.A. Saunders, P.J. Coffer, R.H. Medema, R.C. Coombes, and E.W. Lam. 2003. FoxO3a transcriptional regulation of Bim controls apoptosis in paclitaxel-treated breast cancer cell lines. *J. Biol. Chem.* 278:49795–49805. doi:10.1074/jbc.M309523200
- Suter, M., C. Remé, C. Grimm, A. Wenzel, M. Jäättelä, P. Esser, N. Kociok, M. Leist, and C. Richter. 2000. Age-related macular degeneration. The lipofusion component N-retinyl-N-retinylidene ethanolamine detaches proapoptotic proteins from mitochondria and induces apoptosis in mammalian retinal pigment epithelial cells. *J. Biol. Chem.* 275:39625–39630. doi:10.1074/jbc.M007049200



- Suter, M., U. Riek, R. Tuerk, U. Schlattner, T. Wallimann, and D. Neumann. 2006. Dissecting the role of 5'-AMP for allosteric stimulation, activation, and deactivation of AMP-activated protein kinase. *J. Biol. Chem.* 281:32207–32216. doi:10.1074/jbc.M606357200
- Turski, L., K. Bressler, K.J. Rettig, P.A. Löschmann, and H. Wachtel. 1991. Protection of substantia nigra from MPP+ neurotoxicity by N-methyl-D-aspartate antagonists. *Nature.* 349:414–418. doi:10.1038/349414a0
- Tymianski, M., M.C. Wallace, I. Spigelman, M. Uno, P.L. Carlen, C.H. Tator, and M.P. Charlton. 1993. Cell-permeant Ca<sup>2+</sup> chelators reduce early excitotoxic and ischemic neuronal injury in vitro and in vivo. *Neuron.* 11:221–235. doi:10.1016/0896-6273(93)90180-Y
- Vergun, O., Y.Y. Han, and I.J. Reynolds. 2003. Glucose deprivation produces a prolonged increase in sensitivity to glutamate in cultured rat cortical neurons. *Exp. Neurol.* 183:682–694. doi:10.1016/S0014-4886(03)00243-7
- Villunger, A., E.M. Michalak, L. Coultas, F. Müllauer, G. Böck, M.J. Ausserlechner, J.M. Adams, and A. Strasser. 2003. p53- and drug-induced apoptotic responses mediated by BH3-only proteins puma and noxa. *Science.* 302:1036–1038. doi:10.1126/science.1090072
- Wang, H., S.W. Yu, D.W. Koh, J. Lew, C. Coombs, W. Bowers, H.J. Federoff, G.G. Poirier, T.M. Dawson, and V.L. Dawson. 2004. Apoptosis-inducing factor substitutes for caspase executioners in NMDA-triggered excitotoxic neuronal death. *J. Neurosci.* 24:10963–10973. doi:10.1523/JNEUROSCI.3461-04.2004
- Ward, M.W., A.C. Rego, B.G. Frenguelli, and D.G. Nicholls. 2000. Mitochondrial membrane potential and glutamate excitotoxicity in cultured cerebellar granule cells. *J. Neurosci.* 20:7208–7219.
- Ward, M.W., M. Rehm, H. Duesmann, S. Kacmar, C.G. Concannon, and J.H. Prehn. 2006. Real time single cell analysis of Bid cleavage and Bid translocation during caspase-dependent and neuronal caspase-independent apoptosis. *J. Biol. Chem.* 281:5837–5844. doi:10.1074/jbc.M511562200
- Ward, M.W., H.J. Huber, P. Weisová, H. Duesmann, D.G. Nicholls, and J.H. Prehn. 2007. Mitochondrial and plasma membrane potential of cultured cerebellar neurons during glutamate-induced necrosis, apoptosis, and tolerance. *J. Neurosci.* 27:8238–8249. doi:10.1523/JNEUROSCI.1984-07.2007
- Wei, M.C., W.X. Zong, E.H. Cheng, T. Lindsten, V. Panoutsakopoulou, A.J. Ross, K.A. Roth, G.R. MacGregor, C.B. Thompson, and S.J. Korsmeyer. 2001. Proapoptotic BAX and BAK: a requisite gateway to mitochondrial dysfunction and death. *Science.* 292:727–730. doi:10.1126/science.1059108
- Weisová, P., C.G. Concannon, M. Devocelle, J.H. Prehn, and M.W. Ward. 2009. Regulation of glucose transporter 3 surface expression by the AMP-activated protein kinase mediates tolerance to glutamate excitation in neurons. *J. Neurosci.* 29:2997–3008. doi:10.1523/JNEUROSCI.0354-09.2009
- Whitfield, J., S.J. Neame, L. Paquet, O. Bernard, and J. Ham. 2001. Dominant-negative c-Jun promotes neuronal survival by reducing BIM expression and inhibiting mitochondrial cytochrome c release. *Neuron.* 29:629–643. doi:10.1016/S0896-6273(01)00239-2
- Woods, A., D. Azzout-Marniche, M. Foretz, S.C. Stein, P. Lemarchand, P. Ferré, F. Foufelle, and D. Carling. 2000. Characterization of the role of AMP-activated protein kinase in the regulation of glucose-activated gene expression using constitutively active and dominant negative forms of the kinase. *Mol. Cell. Biol.* 20:6704–6711. doi:10.1128/MCB.20.18.6704-6711.2000
- Xiang, H., Y. Kinoshita, C.M. Knudson, S.J. Korsmeyer, P.A. Schwartzkroin, and R.S. Morrison. 1998. Bax involvement in p53-mediated neuronal cell death. *J. Neurosci.* 18:1363–1373.
- Yakovlev, A.G., K. Ota, G. Wang, V. Movsesyan, W.-L. Bao, K. Yoshihara, and A.I. Faden. 2001. Differential expression of apoptotic protease-activating factor-1 and caspase-3 genes and susceptibility to apoptosis during brain development and after traumatic brain injury. *J. Neurosci.* 21:7439–7446.
- Youle, R.J., and A. Strasser. 2008. The BCL-2 protein family: opposing activities that mediate cell death. *Nat. Rev. Mol. Cell Biol.* 9:47–59. doi:10.1038/nrm2308